ASTRONOMY & ASTROPHYSICS
SUPPLEMENT SERIES

Astron. Astrophys. Suppl. Ser. **123,** 119-133 (1997)

The supercluster–void network

I. The supercluster catalogue and large-scale distribution

M. Einasto[1], E. Tago[1], J. Jaaniste[1], J. Einasto[1], and H. Andernach[2]

[1] Tartu Observatory, EE-2444 Tõravere, Estonia
[2] IUE Observatory, Villafranca, Apartado 50727, E-28080 Madrid, Spain

Received March 4; accepted August 21, 1996

Abstract. We investigate the distribution of superclusters and voids using a new catalogue of superclusters of rich clusters of galaxies which extends up to a redshift of $z = 0.12$. The new catalogue contains 220 superclusters of rich clusters, of which 90 superclusters have been determined for the first time. Among them there are several very rich superclusters, containing at least eight member clusters.

We demonstrate that two thirds of very rich superclusters are concentrated to a Dominant Supercluster Plane which is situated at a right angle with respect to the plane of the Local Supercluster and adjacent nearby superclusters.

We apply several methods to estimate the characteristic distance between superclusters. The results indicate consistently the presence of a quite regular supercluster-void network with scale of ≈ 120 h^{-1} Mpc.

Comparison with random supercluster catalogues shows significant differences between spatial distributions of real and random superclusters.

We determine the selection function of the sample of clusters and suggest that the mean true space density of Abell clusters is $2.6\ 10^{-5}$ h^3 Mpc^{-3}, twice the conventionally used value[1].

Key words: cosmology: observations — large-scale structure of the Universe — clusters of galaxies — catalogs

Send offprint requests to: M. Einasto

[1] Table A2 is only available in electronic form at the Centre des Données astronomiques Strasbourg via anonymous ftp to cdsarc.u-strasbg.fr (130.79.128.5) or via http://cdsweb.u-strasbg.fr/Abstract.html

1. Introduction

Galaxies and systems of galaxies form due to initial density perturbations of different scale. Short perturbations with a wavelength of several Mpc give rise to the formation of individual galaxies and small systems of galaxies, medium scale perturbations lead to the formation of clusters of galaxies, and so on. Perturbations of a characteristic scale of ~ 100 h^{-1} Mpc can be related to superclusters of galaxies. Still larger perturbations have much lower amplitude and thus they only modulate densities and masses of smaller systems (Frisch et al. 1995). Therefore superclusters of galaxies are the largest relatively isolated density enhancements in the Universe.

The presence of superclusters is known since the pioneering studies of Shapley (1930). The nearest example is the Local Supercluster with the Virgo cluster as the central cluster (de Vaucouleurs 1956). Other nearby examples are the Perseus-Pisces supercluster which consists of the Perseus chain of rich clusters, and the Coma supercluster with the Coma cluster and A1367 forming its double center. The distribution of galaxies in superclusters is filamentary, these filaments can contain as density enhancements groups and clusters galaxies of different richness (Gregory & Thompson 1978; Jõeveer et al. 1978; Einasto et al. 1984).

Superclusters are not completely isolated in space. Galaxy and cluster filaments connect neighbouring superclusters to a single network. Filaments joining the Local and Perseus-Pisces superclusters were noticed by Einasto et al. 1980, and filaments joining the Local and Coma superclusters by Zeldovich et al. (1982) and Tago et al. (1984, 1986). A section of the Great Wall (Geller & Huchra 1989) is a filamentary system which joins the Coma and Hercules superclusters (Lindner et al. 1995).

We shall use the term supercluster-void network for the web of filaments, clusters, and voids which extends over the whole observable part of the Universe. The formation of a filamentary web of galaxies and clusters is

predicted in any physically motivated scenario of structure formation (of recent works we mention studies by Bond et al. 1996 and Katz et al. 1996). Properties of this network depend on the density perturbations of medium and large wavelengths. Thus the study of the properties of the supercluster-void network yields information on the shape of the initial power spectrum on these wavelengths. Of particular interest is the region of transition from the Harrison-Zeldovich spectrum with positive power index $n = 1$ on very large scales to galactic scales with negative effective power index $n \approx -1.5$. In this wavelength region differences between various structure formation scenarios are the largest.

Our present series of papers is devoted to the study of the properties of the supercluster-void network. Superclusters can be determined using the appropriately smoothed density field, or using discrete tracers, such as galaxies or clusters of galaxies, and applying the clustering analysis. In both cases superclusters can be defined as the largest non-percolating systems of galaxies or clusters of galaxies. Decreasing the threshold density or increasing the neighbourhood radius we get already a percolating system – the supercluster-void network. Both galaxies and clusters are concentrated to superclusters and trace similar high-density regions of the Universe (Oort 1983; Bahcall 1991). In detail the distributions are different, since clusters of galaxies trace only compact high-density regions – the skeleton of the structure. The use of galaxies as tracers of superclusters is limited to relatively small distances as catalogues of redshifts of galaxies which cover a large fraction of the sky are not deep and complete enough yet. On the contrary, the catalogues of rich clusters of galaxies by Abell (1958) and Abell et al. (1989, ACO), which cover the whole sky out of the Milky Way zone of avoidance, are thought to be fairly complete up to distances of several hundred megaparsecs. Thus most supercluster studies were based on these catalogues of clusters of galaxies.

Catalogues of superclusters using clusters as structure tracers have been compiled by Bahcall & Soneira (1984); Batuski & Burns (1985); West (1989); Postman et al. (1992). The first whole-sky supercluster catalogues were prepared by Zucca et al. (1993, hereafter ZZSV); Einasto et al. (1994, hereafter EETDA); and Kalinkov & Kuneva (1995), the last one uses mainly clusters with estimated redshifts.

In the study of the distribution of superclusters it is of central importance to know whether it deviates from a random distribution, and if yes, whether the supercluster distribution defines a certain scale in the Universe. These questions were addressed already by Oort (1983). Subsequent studies have shown the presence of some regularities in the distribution of superclusters. Zeldovich et al. (1982) and Tully (1986, 1987) demonstrated that nearby superclusters are concentrated to a plane which almost coincides with the plane of the Local Supercluster. This concentration of superclusters forms a wall dividing two huge voids, the Northern and Southern Local voids (Einasto & Miller 1983; Lindner et al. 1995). Tully et al. (1992) showed that several superclusters are almost perpendicular to Local Supercluster plane. EETDA suggested that superclusters and voids form a quite regular network with a characteristic distance between superclusters of about $110 - 140$ h^{-1} Mpc. A similar scale was found by Mo et al. (1992) in the distribution of clusters of galaxies; the value is also close to that found by Broadhurst et al. (1990) for the distance between peaks in the redshift distribution of galaxies in a pencil-beam survey of galaxies and. The scale of about 100 h^{-1} Mpc has also been found in the distribution of QSO absorption line systems (Quashnock et al. 1996). These results suggest the presence of a peak in the power spectrum of density fluctuations at the corresponding wavelength (Einasto & Gramann 1993; Frisch et al. 1995). An excess power in the power spectrum of galaxies of the Las Campanas redshift survey has been detected at this scale by Landy et al. (1996).

In recent years the number of clusters with measured and re-measured redshifts has been increased considerably. Thus a new and more detailed analysis of the distribution of clusters and superclusters is possible. In this series of papers we shall construct a new catalogue of superclusters, study the large-scale distribution of superclusters (the present paper), determine the correlation function and the power spectrum of clusters of galaxies (Einasto et al. 1997a-c), investigate the form and orientation of superclusters (Jaaniste et al. 1997), compare the distribution of clusters and superclusters of galaxies with the distribution of similar objects in numerical simulations (Frisch et al. 1997), and investigate consequences of these results to scenarios of structure formation (Einasto et al. 1997a,b).

The present paper is arranged as follows. Section 2 presents a new catalogue of superclusters up to $z = 0.12$. Redshift data are available for 2/3 of the clusters within this distance limit. We use this limit in order to include very rich superclusters missed in the earlier version of the catalogue (EETDA). In addition, we apply improved distance estimates for clusters without observed redshifts (Peacock & West 1992). In Sect. 3 we determine the selection function and mean space density of clusters. In Sect. 4 we describe catalogues of randomly located superclusters. In Sect. 5 we use the catalogue of superclusters to describe and analyse the structures delineated by superclusters on large scales, and compare the spatial distribution of rich and poor superclusters and isolated clusters. In Sect. 6 we analyse the sizes of voids defined by rich clusters from systems of various richness. In Sect. 7 we calculate the characteristic distance between the largest systems. In Sect. 8 we study the distribution of superclusters of different richness in void walls. Section 9 gives a summary of principal results.

We denote with h the Hubble constant in units of 100 km s^{-1} Mpc^{-1}.

2. The catalogue of superclusters

2.1. The cluster data

The Abell–ACO catalogue includes 2712 northern clusters originally published by Abell (1958), 1364 rich southern clusters that are counterparts to the Abell clusters and 1174 supplementary poor southern clusters (Abell et al. 1989). Some rich clusters are duplications, therefore the combined Abell–ACO catalogue includes at most 4069 rich clusters. In this paper we use only these rich clusters of the Abell–ACO catalogue and call them simply as clusters.

We are updating redshift data for Abell–ACO clusters continuously using all available sources including some unpublished redshifts. The present discussion reflects our dataset as of May 1995. A catalogue of published redshifts and velocity dispersions for Abell–ACO clusters, including supplementary clusters, is in preparation (cf. Andernach et al. 1995). For clusters without observed redshift a photometric estimate of the distance is given using the correlation between redshifts and magnitudes of cluster galaxies (Peacock & West 1992). The errors of estimated redshifts are about 27% for the northern (Abell) and 18% for the southern (ACO) clusters which are considerably higher than errors for spectroscopically measured redshifts. The redshifts have been corrected to the rest frame of the Local Group ($\Delta z = 0.001 \sin l \cos b$) and for the expansion effects. The expansion correction depends on the adopted model and density parameter of the universe. We have used a correction which corresponds to a closed universe ($\Omega_0 + \Omega_\Lambda = 1$) and a value of the density parameter, $\Omega_0 \approx 0.7$. Results depend on the particular value of the density parameter only very weakly.

For a number of clusters published redshifts obviously belong to a foreground or background galaxy (some of them are marked by ACO and Struble & Rood 1991, and also by Dalton et al. 1994). We have used estimated redshifts instead of poorly observed ones if $|\log(z_{\rm obs}/z_{\rm est})| > 0.3$ and if the number of measured galaxy redshifts per clusters was $n_z < 3$. The influence of such clusters on our catalogue will be discussed later.

To compile the supercluster catalogue we extracted from the whole Abell–ACO catalogue a spatially limited sample up to a distance $z = 0.12$. This sample contains 1304 clusters, and includes clusters of all richness classes. Of these clusters 2/3 have measured redshifts. We have included in our study clusters of richness class 0. Arguments for this were already discussed by EETDA. Possible projection effects discussed by Sutherland (1988), Dekel et al. (1989) and others are not crucial for the present study as we are mostly interested in the distribution of clusters on much larger scales (cf. EETDA).

2.2. Supercluster finding procedure

Superclusters have been determined by the clustering (or friends-of-friends) algorithm (Huchra & Geller 1982; Press & Davis 1982; Zeldovich et al. 1982). Clusters are searched for neighbours at a fixed neighbourhood radius; objects having distances between each other less than this radius are collected to a system. We use the same neighbourhood radius as in EETDA, 24 h^{-1} Mpc. EETDA showed that at neighbourhood radii up to about 16 h^{-1} Mpc the cores of individual superclusters start to form; at radii larger than 30 h^{-1} Mpc superclusters begin to join into percolating agglomerates. At the radius of about 24 h^{-1} Mpc superclusters are the largest still relatively isolated density enhancements in the Universe. Our analysis shows that the main results do not change if we use the neighbourhood radius in the interval of $20 - 28$ h^{-1} Mpc.

In some cases the clustering radius used here is too large, and forces clusters to join into large aggregates which probably cannot be considered as single superclusters. One example for this is the Shapley supercluster that will be discussed by Jaaniste et al. (1997).

2.3. The catalogue of superclusters

We include in the catalogue of superclusters all systems with at least two member clusters. We shall use the term *multiplicity* k for the number of member clusters in a supercluster. The distance limit is set at $z = 0.12$; in this volume there are in total 220 superclusters (for the neighbourhood radius 24 h^{-1} Mpc). The distribution of multiplicities of the superclusters in our catalogue is shown in Fig. 1. Here we plot also isolated clusters. Complete data on superclusters having at least four members (multiplicity, centre coordinates, list of member clusters and identifications with previous catalogues) are given in Table A1 in the Appendix, the whole catalogue is presented in electronic form in Table A2. Clusters for which only estimated redshifts are available are appended by a letter e.

A number of superclusters have well-known previous identifications. These are given in Col. (7) of Table A1. Their designations are usually based on the constellation on which the supercluster members are projected. In the case of rich, well-determined superclusters without previous identifications we assigned new identifications using the same system. If there were more than one supercluster projected on the same constellation, we added the letters A, B, and so on (in order of increasing z). Otherwise, if the supercluster members were projected on more than one constellation, we used a double name.

About 1/3 of the clusters in our sample have estimated redshifts only (437 of 1304 clusters). The median distance of clusters with measured redshifts (230 h^{-1} Mpc) is smaller than that of clusters with estimated redshifts (300 h^{-1} Mpc), which reflects the better completeness in redshift measurements for nearer clusters.

In order to see the influence of the use of clusters with estimated redshifts on our catalogue, we performed the cluster analysis using only clusters with measured redshifts. We searched for systems using the same neighbourhood radius as before, 24 h^{-1} Mpc. As a result we obtained a test catalogue of superclusters with 136 systems. All the superclusters containing less than two members with measured redshifts disappeared, of course, after this procedure. However, the remaining superclusters appeared to be surprisingly stable: almost all systems with at least two clusters with measured redshifts were found also in this test catalogue, and only a few clusters with measured redshifts were excluded from systems. One supercluster, the Aquarius supercluster (SCL 205), was split up into two subsystems.

Thus we consider all the superclusters with less than two members with measured redshifts as supercluster candidates. These superclusters have a letter c to its catalogue number. We also marked those clusters with measured redshifts that were eliminated from systems determined by clusters with measured redshifts only, as described above.

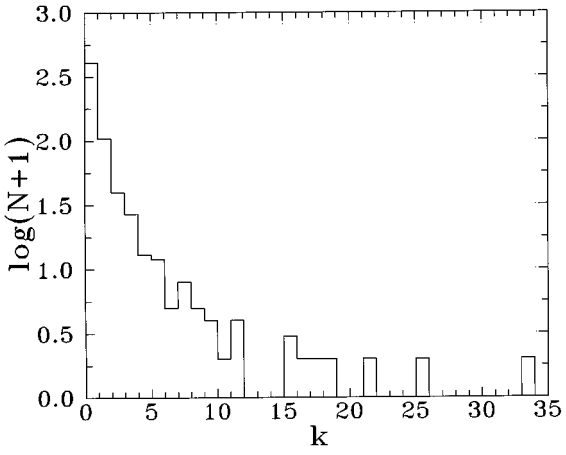

Fig. 1. The distribution of supercluster multiplicities for the neighbourhood radius $R = 24$ h^{-1} Mpc. Isolated clusters ($k = 1$) are included for comparison

Of the 220 systems in the new catalogue, 50 superclusters are identical with superclusters in the previous catalogue, 80 have changed the multiplicity (in most cases these superclusters have gained or lost $1 - 2$ members due to newly measured redshifts). The catalogue contains 25 previously unreported superclusters within the distance of $d < 300$ h^{-1} Mpc; all 65 superclusters beyond 300 h^{-1} Mpc are reported here for the first time. As seen from these numbers, our regular updating of the catalog has lead to a considerable improvement. In addition, our analysis showed that the large scale structures delineated by superclusters from the present and previous catalogues are almost identical in the nearby volume covered by both catalogues.

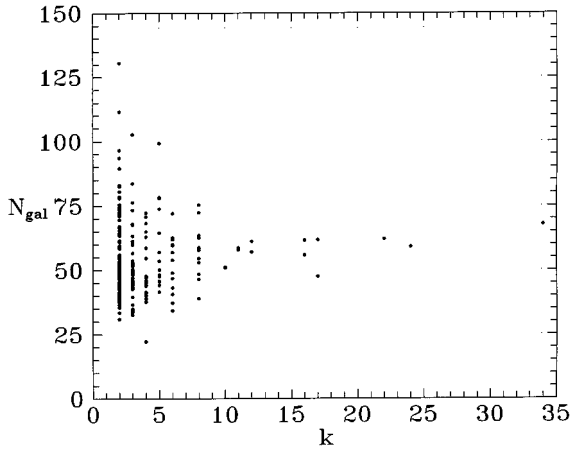

Fig. 2. Mean number of galaxies in clusters belonging to superclusters of multiplicity k

We divide superclusters into several richness classes. We call superclusters with less than 4 members as *poor*, and those with 4 or more members as *rich*. Rich superclusters are divided into subclasses: superclusters with $4 - 7$ members are called as *medium rich*, and those with 8 or more members as *very rich*. About half of the 220 superclusters of the catalogue are cluster pairs; the catalogue contains 53 medium rich superclusters, and 25 very rich superclusters. Very rich superclusters represent the regions of the highest density in the Universe. They contain 25% of all clusters and over 30% of all supercluster members. Of these very rich superclusters 4 have been catalogued for the first time. These are the Draco (SCL 114, $k = 16$), the Caelum (SCL 59_c, $k = 11$), the Bootes A (SCL 150, $k = 10$), and the Leo – Virgo (SCL 107, $k = 8$) superclusters. In the following sections we shall compare the spatial distribution of superclusters of different richness.

Supercluster masses are evidently larger when they contain more galaxies. To check the relationship between the supercluster richness and the number of galaxies contained in a supercluster we plot in Fig. 2 the mean number of galaxies in superclusters against supercluster multiplicity. We used the Abell count of galaxies (C in ACO) as the number of galaxies per cluster. Clearly, the mean number of galaxies in clusters located in superclusters of different multiplicity is practically constant. This test shows that the supercluster multiplicity is an indicator of the mass of the supercluster (see also Frisch et al. 1995). An example supported by actual observations is the Shapley supercluster, the richest supercluster in our catalogue. It contains the richest clusters in the volume under study and a large number of X-ray emitting clusters which indicate the

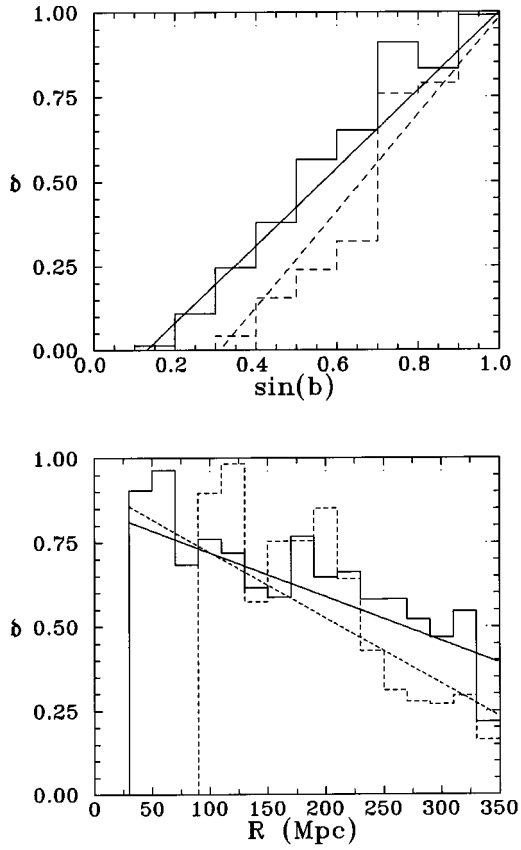

Fig. 3. Selection functions for clusters. In the upper panel the density of clusters is shown as a function of the galactic latitude, $\sin b$, in the lower panel as a function of distance from the observer, r. Solid histograms are for all clusters, dashed histograms for clusters in very rich superclusters. Straight lines show the linear approximation of the selection function. The curves are normalised to 1 for the galactic poles and for zero distance to the observer

presence of a deep potential well in this supercluster (Breen et al. 1994; EETDA).

2.4. Notes on very rich superclusters

First we give some notes on previously known superclusters.

The *Shapley supercluster* (SCL 124), first described by Shapley in (1930), is certainly the most prominent supercluster in the region under study (ZZSV). This supercluster contains the richest Abell clusters in the area studied, and a number of X-ray clusters (Quintana et al. 1995 and references therein). This supercluster is located approximately 140 h^{-1} Mpc from us, bordering the farther side of the Northern Local void (EETDA, Lindner et al. 1995).

The *Virgo–Coma supercluster* (SCL 111) with 16 members forms a wall between two voids. Of these 16 clusters 6 have estimated redshifts about 1.5 times larger than are their (poorly) observed redshifts. Thus a possible alternative interpretation of the data is that some of the clusters are more distant, and the measured redshifts belong to foreground galaxies in the region of this supercluster. If we discard these clusters then the supercluster contains at least 8 members and still meets our criterion for very rich superclusters.

The *Horologium–Reticulum supercluster* (SCL 48), the longest and the second richest supercluster in the previous catalogue, has been split into subsystems containing now 26 members instead of 32 (EETDA) (see Table 1), being still the second most rich supercluster in the new catalogue but not the longest one (Jaaniste et al. 1997).

Now we comment on those very rich superclusters ($k \geq 8$) in our catalogue which were not previously reported.

The *Draco supercluster* (SCL 114) has 16 members, all with measured redshifts, being one of the richest superclusters in the region under study. The Draco supercluster lies at a distance of 300 h^{-1} Mpc on a side of a void of diameter of about 130 h^{-1} Mpc, the near side of which is determined by the Ursa Majoris supercluster. The Draco supercluster is one of the most isolated very rich superclusters in our catalog. However, being located near the distance limit of our sample this supercluster might have a neighbour farther away. The shape of this supercluster resembles a pancake with axis ratios 1:4:5 (Jaaniste et al. 1997).

The *Bootes A supercluster* (SCL 150) borders a giant void on the farther side of the Bootes supercluster which separates this void from the Bootes void. Nine of the ten members of this supercluster have measured redshifts.

The *Leo–Virgo supercluster* (SCL 107) has 8 members, six of them have measured redshifts. This supercluster borders the same void as SCL 111.

The *Caelum supercluster candidate* (SCL 59c) borders the same void as the Fornax–Eridanus supercluster and is seen in Fig. 3 by Tully et al. (1992) as a density enhancement. However, a word of caution is needed: only two of the 11 members of this supercluster have measured redshifts.

The *Fornax–Eridanus supercluster candidate* (SCL 53c) too consists mostly of clusters with estimated redshifts. The multiplicity of this supercluster may change when new redshift data for rich clusters in this region become available.

3. Selection functions and the mean volume density of clusters

In this section we study the influence of selection effects on the distribution of clusters and superclusters, and on the space density of clusters.

The probability to detect a cluster at a certain location depends on the galactic obscuration and on the distance of the cluster. To investigate the selection effects we determined the volume density of clusters of galaxies in bins of

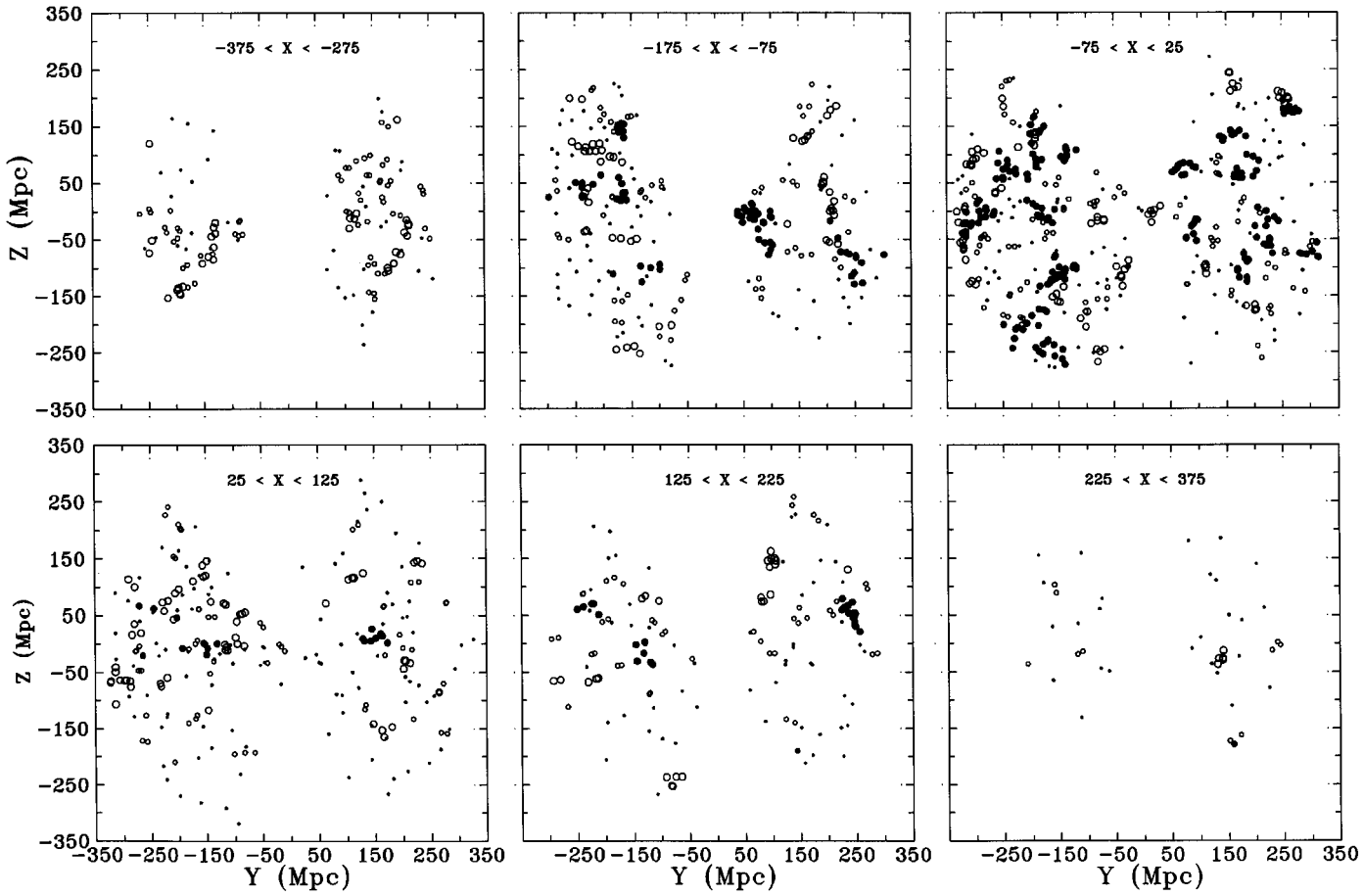

Fig. 4. The distribution of clusters in supergalactic coordinates in slices of thickness $d = 100$ h^{-1} Mpc in the supergalactic X direction. Clusters belonging to very rich superclusters are denoted with filled circles; clusters, belonging to medium rich superclusters – with empty circles, and isolated clusters and members of poor superclusters are plotted with small dots. The first and last slices are thicker since due to the use of the spherical volume outlying slices contain less clusters

spherical shells of thickness of 20 h^{-1} Mpc and in bins of $\Delta \sin b = 0.1$ (b is the galactic latitude). Results are shown in Fig. 3, separately for all clusters and for the population of clusters in very rich superclusters with at least 8 members. The distributions are given for all clusters, but the selection effects are similar for only the clusters with measured redshifts (Einasto et al. 1997b).

This figure shows that the dependence of the space density of clusters on distance and on $\sin b$ is almost linear. Thus we can represent the selection effects by linear laws: $D(r) = d_0 - d_1(r/r_1)$, and $D(\sin b) = s_0 + s_1 \sin b$, where d_0, d_1, s_0, and s_1 are constants, and r_1 is the limiting radius of the sample. Both for *all* clusters and for those in *very rich* superclusters, corrected for incompleteness and Galactic extinction, we find: $d_0 = 1$, $d_1 = 0.5$. The latitude dependence is given by the value $s_0 = \sin b_0$, at which the density is equal to zero. For samples of all clusters and clusters in very rich superclusters we get $s_0 = 0.12$, and $s_0 = 0.38$, respectively.

These data were used also to derive the mean number density of clusters in space. In order to be left with 1304 clusters in the volume under investigation and with the above selection function, we actually need approximately 9000 clusters in a cube of side 700 h^{-1} Mpc. Thus the mean density of Abell–ACO clusters in space, corrected for incompleteness and Galactic extinction, is 26 per cube of side-length 100 h^{-1} Mpc, or 2.6 10^{-5} h^3 Mpc^{-3}, or approximately twice the estimate by Bahcall & Cen (1993). This estimate of the space density of clusters is consistent with the results by Postman et al. (1996) obtained from the study of distant clusters.

This calculation shows that selection effects are important in deriving the density of clusters in space. The comparison with random supercluster catalogues also shows that in low galactic latitudes the multiplicity of superclusters is distorted as some supercluster members are not visible. This explains the observed fact that the density of rich and very rich superclusters decreases toward galactic

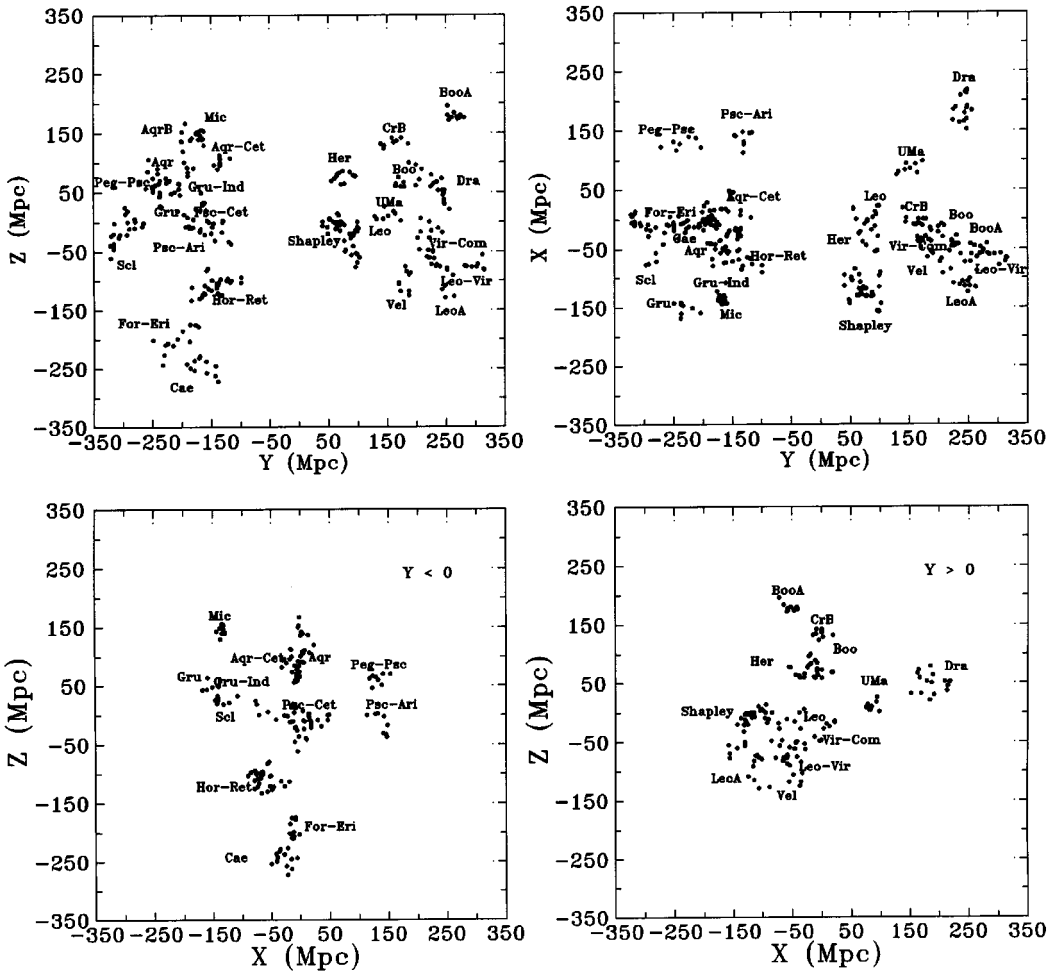

Fig. 5. The distribution of clusters belonging to very rich superclusters in supergalactic coordinates. Supercluster identifications are given

equator more rapidly than the density of poor superclusters, see Fig. 3.

4. Random supercluster catalogues

In order to compare the spatial distribution of clusters and superclusters with random distributions and to investigate the influence of the selection effects on the number density of clusters we generated two sets of randomly located superclusters.

In both sets the number of clusters was the same as in the observed catalogue (approximately 1300), they occupy the same volume, and are combined into superclusters that have multiplicity distribution similar to that of real superclusters. First we generated supercluster centres, and then supercluster members around each centre. The radius of superclusters was chosen in accordance with observations: 10 h^{-1} Mpc and 20 h^{-1} Mpc, for poor and rich superclusters, respectively (EETDA, Jaaniste et al. 1997). Clusters outside the sphere of radius, $r > r_1$, and near the Galactic plane, $|\sin b| < \sin b_0$, were excluded. The selection effects were taken into account in two different ways.

In the first set of random catalogues centres of superclusters and locations of isolated clusters were generated using a censored random distribution: in order to avoid overlapping of the superclusters a minimum distance of 40 h^{-1} Mpc was chosen between these centres and a minimum distance of 24 h^{-1} Mpc was chosen between clusters that did not belong to the superclusters, as in the case of real isolated clusters. This set of random supercluster catalogues was generated without taking into account detailed selection effects (i.e. clusters were absent from the zone of avoidance but the changes in the mean density of clusters in distance and in galactic latitude were ignored).

In the second set of random catalogues we took into account the selection functions derived from the observed sample of all clusters. The locations of the supercluster centres and isolated clusters were generated completely randomly, the number of members for each supercluster was generated according to both the multiplicity function

of real superclusters, and to the selection functions which determined the probability to find a cluster at a given galactic latitude and distance from the observer. The number of clusters that were generated but not included to the catalogue due to selection effects gives us an estimate of the real number of clusters in the volume under study (see the previous section). The final multiplicity of superclusters was determined using the clustering algorithm and a neighbourhood radius of 24 h^{-1} Mpc.

To check the validity of the selection function procedures we calculated the density distribution of clusters for both sets of random supercluster catalogues. As expected, the dependence of the cluster density on the galactic latitude and distance was similar to the observed one in the case of the second set of random catalogues, while in the case of the first set this dependence was much weaker. The multiplicity distribution of superclusters for the second set of models was almost identical to the multiplicity distribution in the real catalogue. We shall discuss the influence of differences in the selection function on the tests applied in the present paper in corresponding sections.

5. Distribution of superclusters

In this section we study the overall distribution of superclusters. In Figs. 4 and 5 we show the distribution of clusters in supergalactic coordinates. In Fig. 4 all clusters are plotted in slices of 100 h^{-1} Mpc thickness. In Fig. 5 we plot only clusters belonging to very rich superclusters, in the lower panels of this figure clusters from the Southern and Northern sky are given separately. Clusters with estimated redshifts (members of the supercluster candidates) are also included.

Figures 4 and 5 show that the network of superclusters and voids extends over the entire volume displayed. Superclusters are separated by huge voids. For example, the Hercules (SCL 160) and the Shapley (SCL 124) superclusters border the Northern Local void; the Hercules, the Bootes (SCL 138) and the Corona Borealis (SCL 158) superclusters surround the Bootes void, that is bordered by the Draco supercluster (SCL 114) in its far side. In the Southern sky the Sculptor supercluster (SCL 9) forms the farther wall of the Sculptor void, to name only the most well–known voids.

The distribution of X-ray emitting clusters from the ROSAT survey (Romer et al. 1994) shows essentially the same structures. The excess of ROSAT clusters in the region of the Pisces–Cetus supercluster and in the Sculptor wall are seen particularly well.

5.1. Supercluster sheets and chains

Figures 4 and 5 suggest that superclusters are not distributed homogeneously. Most of very rich superclusters are located along rods of a quasi-regular rectangular cubic lattice with almost constant step, and form elongated structures – chains. These chains are almost parallel to axes of supergalactic coordinates. The whole distribution of clusters along rods is essentially one-dimensional. One possibility to give a quantitative description of the supercluster chains is to use the fractal dimension, $D = 3 - \gamma$, where γ is the slope of the correlation function expressed in log−log form (Coleman & Pietronero 1992). On small scales the slope of the cluster-cluster correlation function characterises the fractal dimension of superclusters themselves, on larger scales up to about 90 h^{-1} Mpc the slope is determined by the shape of supercluster systems. On these scales the fractal dimension determined for all clusters is $D_{\rm all\ cl} \approx 2$. This value coincides well with the correlation fractal dimension for galaxies on large scales outside clusters (Einasto 1991; Di Nella et al. 1996). The correlation fractal dimension calculated for clusters that belong to very rich superclusters is smaller, $D_{\rm scl8} \approx 1.4$. Thus structures delineated by very rich superclusters are more one-dimensional than two-dimensional as in the case of structures defined by all clusters.

Several data sets suggest that giant structures seen in the Southern and Northern sky may be connected, and superclusters form sheets or planes in supergalactic coordinates. One example of such connection is the Supergalactic Plane, which contains the Local Supercluster, the Coma Supercluster, the Pisces–Cetus and the Shapley superclusters (Einasto & Miller 1983; Tully 1986 and 1987; Tully et al. 1992, EETDA). This aggregate separates two giant voids – the Northern and the Southern Local supervoids (EETDA).

The search of galaxies in the zone of avoidance has provided further evidence that some other very rich superclusters may be connected through the zone of avoidance. Kraan-Korteweg et al. (1995) found that there may be a chain of galaxies in the zone of avoidance forming a bridge between the Shapley concentration and the Horologium–Reticulum supercluster. This bridge, if real, borders the Southern Local supervoid and connects chains of superclusters parallel to the Supergalactic plane.

5.2. The Dominant supercluster plane

The visual impression from Fig. 5 is that the upper right panel (sheet $-75 \leq X \leq 25$ h^{-1} Mpc) contains most of the members of rich superclusters. No such concentration is seen along other coordinates although we see several peaks in the distribution of clusters in both Z- and Y-directions. We checked this quantitatively by calculating the distribution of member clusters of very rich superclusters along supergalactic coordinates (Fig. 6). In this way we can see whether the clusters are concentrated in a certain supergalactic interval (this approach was chosen because of simplicity and also because several rich systems of superclusters are located almost parallel to one or another plane of supergalactic coordinate axes). The presence of the zone of avoidance causes the absence of

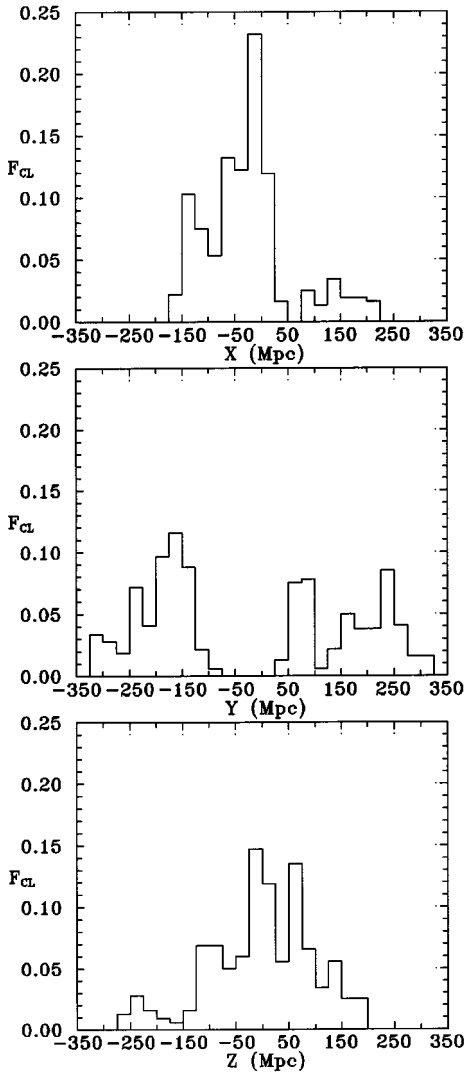

Fig. 6. The distribution of member clusters of very rich superclusters along supergalactic coordinates X, Y, and Z

clusters around $Y = 0$, therefore we can only compare the distributions of clusters along the X and Z coordinates. In the case of uniform distribution the distribution of clusters and superclusters along X and Z axes should be statistically identical. However, the Kolmogorov–Smirnov test shows that the zero hypothesis (distribution of clusters along X and Z coordinates is identical) is rejected at the 99% confidence level.

We compared the distribution of the members of very rich superclusters from real and random catalogues. The results show that of the 320 member clusters of observed very rich superclusters 198 belong to the sheet $-75 \leq X \leq 25\ \mathrm{h}^{-1}$ Mpc. In the case of randomly located superclusters the expected number of clusters in very rich superclusters in the sheet is 80 if we do not take into account the selection effects, and 123, if the selection effects have been taken into account. Therefore no such concentration of clusters is seen in the case of randomly located superclusters.

The evidence that the structures may be connected through the zone of avoidance leads us to believe that superclusters in this supergalactic X interval form a *Dominant Supercluster Plane*. The figures show that this plane is almost perpendicular to the X-axis and crosses the Supergalactic plane almost at right angle.

In fact, already Tully et al. (1992) noted the presence of the supercluster structures that are almost orthogonal to the Supergalactic plane. Due to that they described the supercluster-void network as a *three-dimensional chessboard*. Our data show that structures delineated by rich superclusters are not only orthogonal but also located quite regularly (Sects. 6 and 7). Thus, although the description as a chessboard is a simplification it describes certain aspects of the supercluster-void network rather well.

We list the superclusters belonging to the Dominant Supercluster Plane: the Aquarius–Cetus, the Aquarius, the Aquarius B, the Pisces–Cetus, the Horologium–Reticulum, the Sculptor, the Fornax–Eridanus and the Caelum superclusters in the Southern sky, and the Corona Borealis, the Bootes, the Hercules, the Virgo–Coma, the Vela, the Leo, the Leo A, the Leo–Virgo and the Bootes A in the Northern sky. These superclusters do not form a featureless wall – the Dominant Supercluster Plane is formed by a number of intertwined chains of rich superclusters.

5.3. The distribution of poor superclusters and isolated clusters

We showed that very rich superclusters are arranged in chains and walls, separated by huge voids. To study the distribution of poor superclusters and isolated clusters with respect to richer superclusters we used the nearest neighbour test as in EETDA. In this test we calculate the distribution of distances of the nearest neighbours between members of poor superclusters and isolated clusters, and clusters belonging to rich superclusters, and the distribution of distances between randomly located points and clusters from rich superclusters. In this way we can see whether these clusters are located close to rich superclusters, or they form a more or less randomly distributed smooth population in voids.

In order to obtain a hypothetical homogeneous void population we generated a sample of random clusters which are located at a distance $d > 24\ \mathrm{h}^{-1}$ Mpc from real clusters that belong to rich superclusters and occupy the same volume as real clusters. The number of these random clusters was equal to the number of isolated clusters and poor supercluster members.

The results of this test are shown in the Fig. 7. We see that the nearest neighbour distribution curves of these sample pairs deviate from each other – real isolated clusters and members of poor superclusters are located much

closer to rich superclusters than randomly located test clusters. A Kolmogorov-Smirnov test shows that these distributions are different at the 99% confidence level. In other words, isolated clusters and clusters in poor superclusters belong to outlying parts of superclusters and do not form a random population in voids.

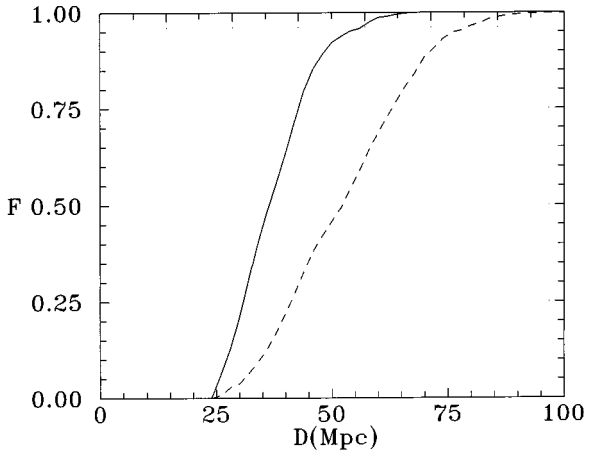

Fig. 7. The integral probability distribution of the nearest neighbour distances: cross distributions for the sample pairs of clusters from rich superclusters vs. isolated clusters (solid curve) and clusters from rich superclusters vs. random points (dashed curve)

6. The sizes of voids between superclusters

To calculate the sizes of voids between clusters and superclusters we used the *empty sphere method*. In this method we divide the cubic sample volume into n^3 cubic cells, where n is a resolution parameter. For each cell centre we determine the distance to the nearest cluster. Cells having the largest distances to the nearest clusters are located in centres of voids. The distances to nearest clusters correspond to the radii of voids. Therefore we obtain the void centre coordinates and radii. For details of the method see Einasto et al. (1989, EEG) and EETDA.

We determined the diameters of voids, delineated by all clusters, by supercluster members, and by members of rich superclusters (Table 1). The number of clusters in these samples is 1304, 900, and 580 clusters, respectively, and samples are denoted as Acl, Asc2, and Asc4 (A stands for Abell). In order to see the influence of the change of the number of clusters on the void sizes we used randomly diluted cluster samples, i.e. from the observed sample (Acl) we removed clusters in a random way so that in the resulting sample the number of clusters was 900 and 580 (correspondingly Ard900 and Ard 580, rd stands for random dilution).

Additionally, we calculated void sizes for random supercluster catalogues. Here again we used samples of all clusters, all supercluster members and members of rich superclusters (correspondingly the samples Rcl, Rsc2, and Rsc4). We used ten realizations of random catalogues. Although this number is rather small, the results for random catalogues are seen quite well. The median diameters of voids for these catalogues are also given in the Table 1. Since the results of void analysis for both sets of random supercluster catalogues were essentially the same, we give in this table the diameters of voids for only one set, the censored random catalogues.

Table 1 shows that the median void sizes in the case of observed cluster and supercluster samples are very close to each other. Also the scatter of void diameter values is rather small (see Fig. 8 in EETDA). We see only a slight increase of void sizes as we move from the sample of all clusters to the supercluster members and to the members of rich superclusters. The reason for the increase of void sizes is clear: although isolated clusters and poor superclusters are located close to void walls, some of them enter into voids determined by rich superclusters, and thus voids determined by all clusters are smaller – the sizes of voids are determined by the location of clusters in the periphery of voids. If we remove clusters in a random way then of course we remove part of the clusters from the central regions of void walls that have no effect to void sizes. Thus the increase of void sizes in this case is smaller than in the first case. Real rich superclusters form a quasi-regular lattice which is almost identical for supercluster samples of all richness classes; much stronger random dilution is needed to destroy this lattice.

Comparison with the random catalogues shows that if the clusters and superclusters are located randomly then the removal of part of the clusters increases the void sizes much more than in the observed case.

7. The characteristic distance between superclusters

We saw that superclusters form intertwined systems that are separated by giant voids of almost equal size. The characteristic scale of this network can be calculated as a distance between centres of superclusters on opposite sides of void walls.

We shall determine distances between high-density regions across the voids using the *pencil-beam* analysis of mean distances between high-density regions, as described by EEG. The volume under study was divided in one direction into n^2 beams. This procedure was repeated in all three directions of coordinate axes, therefore the total number of beams was $3n^2$. In each beam we used cluster analysis to determine density maxima and derived the mean distance between two consecutive density maxima. As a result we obtained the mean distance between superclusters – the mean value over voids in all beams. We used the neighbourhood radius $r = 24\ \mathrm{h}^{-1}$, and two resolutions: $n = 24$ and $n = 12$. The lower resolution was used

Table 1. Median diameters of voids

$N_{\rm cl}$	Sample	$D_{\rm med}$ h^{-1} Mpc	Sample	$D_{\rm med}$ h^{-1} Mpc	Sample	$D_{\rm med}$ h^{-1} Mpc
1304	Acl	90			Rcl	88 ± 6
900	Asc2	100	Ard900	94 ± 5	Rsc2	144 ± 26
580	Asc4	110	Ard580	102 ± 9	Rsc4	173 ± 20

Table 2. Median distances between high-density regions

$N_{\rm cl}$	Sample	$D_{\rm med}$ h^{-1} Mpc	Sample	$D_{\rm med}$ h^{-1} Mpc	Sample	$D_{\rm med}$ h^{-1} Mpc
1304	Acl	122 ± 26			Rcl	143 ± 17
900	Asc2	126 ± 27	Ard900	120 ± 15	Rsc2	$[139 \pm 35]$
580	Asc4	$[116 \pm 18]$	Ard580	122 ± 18	Rsc4	$[140 \pm 33]$

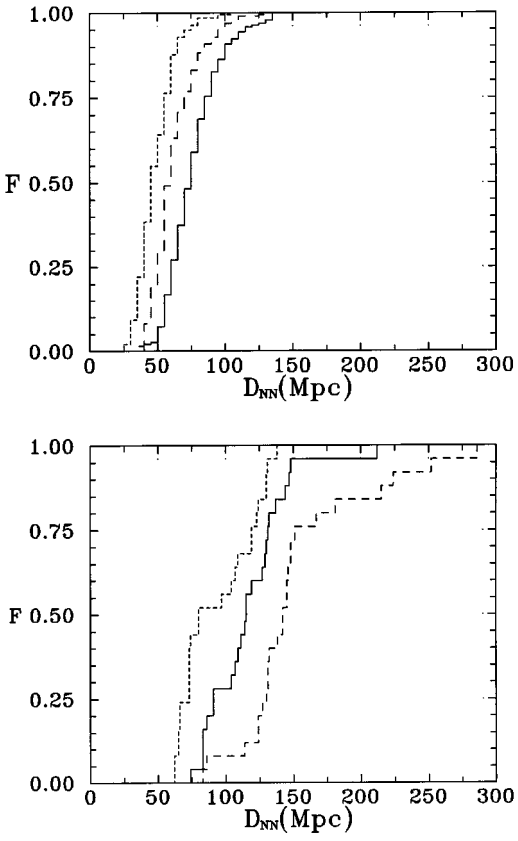

Fig. 8. The distribution of distances between centres of superclusters. Upper panel shows the distributions for poor and medium rich superclusters, lower panel - for the very rich superclusters. Curves correspond to the first (line with short dashes), second (line with long dashes) and third (solid line) neighbour

in the case of subsamples with smaller number of clusters as will be described below. To eliminate the influence of the zone of avoidance we performed calculations separately for the Northern and Southern sky. This method finds mean distances between systems independently of the supercluster definition given in Sect. 3. If the number of systems becomes smaller then also the number of pencil-beams with systems detected in them becomes smaller. In that case we performed pencil-beam analysis with a lower resolution, these results are given in parenthesis.

Table 2 shows the results of our calculations. Mean distances between high-density regions are given for the observed samples Acl, Asc2, and Asc4, as well as for diluted samples Ard900 and Ard580, and for random supercluster samples (first set of random samples) Rcl, Rsc2, and Rsc4 (the number of very rich superclusters in the volume under study is too small to determine distances between them using the pencil-beam method). The table shows that the distances between systems for observed samples almost do not change. This is understandable: in pencil-beams method we determine the positions of the density maxima, and the presence of clusters in low-density regions does not influence the results of this analysis. Thus the mean separation of high-density regions across voids is almost identical for all observed samples. The same occurs in the case of randomly located superclusters, only in this case distances between high-density regions are larger, and the number of detected systems is about three times smaller than in the real case (most beams cross none or only one high-density region and no distance can be derived).

We can compare the last result with the direct estimate of the characteristic distance between high-density regions using void diameters determined above. The median diameter of voids delineated by members of superclusters was about $100\ h^{-1}$ Mpc. If we add the mean size

of the shortest axis of the superclusters, 20 h^{-1} Mpc (EETDA, Jaaniste et al. 1997) then we have as a distance between supercluster centres across the voids a value of 120 h^{-1} Mpc, close to that found using pencil-beam analysis.

We see that several tests indicate the presence of a characteristic scale of about 120 h^{-1} Mpc in the distribution of rich clusters and superclusters of galaxies. This scale corresponds to the distance between superclusters across the voids. The small scatter of this distance enables us to say that the supercluster-void network is rather regular. The present paper confirms the results by EETDA based on a smaller dataset. This characteristic scale is much larger than the typical scale of voids determined by galaxies (Lindner et al. 1995), and is a manifestation of the hierarchy of the distribution of galaxies and voids. Our data suggest also that there exists no larger preferred scale in the Universe (cf. also EETDA). Thus the scale determined by the network of superclusters and voids should be the upper end of the hierarchy of the distribution of galaxies.

We shall discuss theoretical consequences of the presence of such a scale in further papers of this series (Einasto et al. 1997b; Frisch et al. 1997).

8. Distribution of superclusters in void walls

Previous analysis has shown that the sizes of voids determined by members of superclusters of different richness are almost identical. This result, and the absence of a randomly located population of clusters in voids, suggest that practically all clusters are located in void walls, and the overall distribution of superclusters of different richness is rather similar. Now we shall study the distribution of superclusters of different richness in void walls. For that we calculate for each supercluster centre the distances to the centres of three nearest superclusters, separately for poor and medium rich, and for very rich superclusters (Fig. 8).

On the upper panel of Fig. 8 these distributions are given for poor and medium rich superclusters. We see, first, that these distances are small, and second, that these distributions are smooth and do not show the presence of any preferred distance between superclusters (that would be seen as a peak in the distance distribution). The median distances to the first, second and third neighbours are, correspondingly, $D_{\rm NN1} = 45$, $D_{\rm NN2} = 60$ and $D_{\rm NN3} = 75$ h^{-1} Mpc.

In the case of poor and medium rich superclusters from random catalogues the median distances to the first, second and third neighbours are closer to each other than in the observed case: $D_{\rm NN1} = 60 \pm 3$, $D_{\rm NN2} = 63 \pm 3$ and $D_{\rm NN3} = 70 \pm 1$ h^{-1} Mpc.

The distributions of distances between very rich superclusters (Fig. 8, lower panel) are quite different. None of these distributions is smooth as in the upper panel. The most important feature in this figure is the presence of a peak in the distribution of distances of the second and third neighbour in the interval $110 < D_{\rm NN2,3} < 150$ h^{-1} Mpc – over 75% of very rich superclusters have a neighbour at this distance. The median distances to the second and third neighbours are, correspondingly, $D_{\rm NN2} = 115$ and $D_{\rm NN3} = 142$ h^{-1} Mpc. These values are close to the size of voids between superclusters.

Since the number of very rich superclusters is small, it is easy to check to which supercluster pairs these distances correspond. This analysis confirms that the peak in the distribution of the second and third neighbour is due to the pairs of superclusters on opposite sides of void walls.

Also, this analysis shows that about half of the very rich superclusters have their first nearest very rich neighbour at the same side of the void (examples of such pairs are the Fornax-Eridanus and the Caelum superclusters, the superclusters in the Aquarius complex and others) at a distance less than $D_{\rm NN1} = 75$ h^{-1} Mpc.

One can argue that the last result may simply be due to the small number of very rich superclusters. Thus we performed the same analysis with superclusters from random catalogues. In this case the distributions of neighbour distances for superclusters of all richnesses are smoothly increasing without any strong peak as in the observed case for very rich superclusters. The median distances between centres of randomly located very rich superclusters are: $D_{\rm NN1} = 94 \pm 19 h^{-1}$ Mpc, $D_{\rm NN2} = 138 \pm 12 h^{-1}$ Mpc, and $D_{\rm NN3} = 180 \pm 16 h^{-1}$ Mpc, values that are much larger than in the observed case.

This test shows that the overall distribution of superclusters of various richnesses is rather similar, but the distribution of superclusters in void walls depends on the supercluster richness.

Additional evidence for differences in the distribution of poor and rich superclusters comes from the analysis of the correlation function of clusters of galaxies (Einasto et al. 1997b).

9. Conclusions

The main results of our analysis of the spatial distribution of rich clusters and superclusters are:

- we present a new whole-sky catalogue of superclusters of Abell-ACO clusters up to distances $z = 0.12$ which contains 220 superclusters, 90 of which have been determined for the first time. There are several new very rich superclusters with eight or more member clusters;
- about 2/3 of very rich superclusters are located in the Dominant Supercluster plane that is orthogonal to the Supergalactic plane;
- several tests suggest the presence of a characteristic scale of about 120 h^{-1} Mpc in the distribution of clusters and superclusters of galaxies;
- rich superclusters reside in chains and walls;
- the distribution of superclusters in void walls depends on the supercluster richness;

– the mean space density of Abell-ACO clusters of galaxies, corrected for incompleteness and Galactic extinction, is 2.610^{-5} h^3 Mpc^{-3}.

Acknowledgements. This work was partly supported by the Estonian Science Foundation (grant 182) and by the International Science Foundation (grant LDC 000). JJ would like to thank Division of Astronomy and Physics of Estonian Academy of Sciences for financial support. We thank Drs. V. Müller, E. Saar and D. Tucker for fruitful discussions.

References

Abell G., 1958, ApJS 3, 211
Abell G., Corwin H., Olowin R., 1989, ApJS 70, 1 (ACO)
Andernach H., Tago E., Stengler-Larrea E., 1995, Astroph. Lett Comm. 31, 27
Bahcall N.A., 1991, ApJ 376, 43
Bahcall N.A., Cen R., 1993, ApJ 407, L49
Bahcall N.A., Soneira R.M., 1984, ApJ 277, 27
Batuski D.J., Burns J.O., 1985, AJ 90, 1413
Bond J.R., Kofman L., Pogosyan D., 1996, Nat 380, 603
Breen J., Raychaudhury S., Forman W., Jones C., 1994, ApJ 424, 59
Broadhurst T.J., Ellis R.S., Koo D.C., Szalay A.S., 1990, Nat 343, 726
Coleman P.H., Pietronero L., 1992, Phys. Rep. 213, 311
Dalton G.B., Efstathiou G., Maddox S.J., Sutherland W.J., 1994, MNRAS 263, 151
Dekel A., Blumenthal G.R., Primack J.R., Olivier S., 1989, ApJ 338, L5
de Vaucouleurs G., 1956, Vistas Astron. 2, 1584
Di Nella H., Montouri M., Paturel G., Pietronero L., Sylos-Labini F., 1996, A&A 308, L33
Einasto J., Einasto M., Gottlöber S., et al., 1997a, Nat 385, 139
Einasto J., Einasto M., Gramann M., 1989, MNRAS 238, 155 (EEG)
Einasto J., Einasto M., Frisch P., et al., 1997b (submitted to MNRAS)
Einasto J., Einasto M., Frisch P., et al., 1997c (submitted to MNRAS)
Einasto J., Gramann M., 1993, ApJ 407, 443
Einasto J., Jõeveer M., Saar E., 1980, MNRAS 193, 503
Einasto J., Klypin A., Saar E., Shandarin S., 1984, MNRAS 206, 529
Einasto J., Miller R.H., 1983, Early evolution of the Universe and its Present Structure. In: Abell G.O. & Chincarini G. (eds) p. 405
Einasto M., 1991, MNRAS 252, 261
Einasto M., Einasto J., Tago E., Dalton G.B., Andernach H., 1994, MNRAS 269, 301 (EETDA)
Frisch P., Einasto J., Einasto M., Freudling W., Fricke K.J., Gramann M., Saar V., Toomet O., 1995, A&A 296, 611
Frisch P., et al., 1997 (in preparation)
Geller M.J., Huchra J.P., 1989, Sci 246, 897
Gregory S.A., Thompson L.A., 1978, ApJ 222, 784
Huchra J.P., Geller M.J, 1982, ApJ 257, 423
Jaaniste J., Tago E., Einasto M., Einasto J., Andernach H., 1997 (in preparation)
Jõeveer M., Einasto J., Tago E., 1978, MNRAS 185, 357
Kalinkov M., Kuneva I., 1995, A&AS 113, 451
Katz N., Weinberg D.H., Miralda-Escude J., Hernquist L., 1996, ApJ 457, L57
Kraan–Korteweg R.C., Fairall A.P., Balkowski C., 1995, A&A 297, 617
Landy S.D., Shectman S.A., Lin H., Kirshner R.P., Oemler A.A., Tucker D., 1996, ApJ 456, L1
Lindner U., Einasto J., Einasto M., Freudling W., Fricke K.J., Tago E., 1995, A&A 301, 329
Mo H.J., Deng Z.G., Xia X.Y., Schiller P., Börner G., 1992, A&A 257, 1
Oort J.H., 1983, ARA&A 21, 373
Peacock J., West M.J., 1992, MNRAS 259, 494
Postman M., Huchra J., Geller M., 1992, ApJ 384, 404
Postman M., Lubin L.M., Gunn J.E., Oke J.B., Hoessel J.G., Schneider D.P., Christensen J.A., 1996, AJ 111, 615
Press W.H., Davis M., 1982, ApJ 259, 449
Quashnock J.M., Vanden Berk D.E., York D.G., 1996, ApJL 472, L69 (SISSA astro-ph/9609013)
Quintana H., Ramirez A., Melnick J., Raychaudhury S., Slezak E., 1995, AJ 110, 463
Romer A.K., Collins C.A., Böhringer H., Cruddace R.G., Ebeling H., MacGillivray H.T., Voges W., 1994, Nat 372, 75
Shapley H., 1930, Harvard Obs. Bull. 874, 9
Struble M.F,. Rood H.J., 1991, ApJS 77, 363
Sutherland W., 1988, MNRAS 234, 159
Tago E., Einasto J., Saar E., 1984, MNRAS 206, 559
Tago E., Einasto J., Saar E., 1986, MNRAS 218, 177
Tully R.B., 1986, ApJ 303, 25
Tully R.B., 1987, ApJ 323, 1
Tully R.B., Scaramella R., Vettolani G., Zamorani G., 1992, ApJ 388, 9
West M., 1989, ApJ 347, 610
Zeldovich Ya.B., Einasto J., Shandarin S.F., 1982, Nat 300, 407
Zucca E., Zamorani G., Scaramella R., Vettolani G., 1993, ApJ 407, 470 (ZZSV)

Appendix

Table A1. The list of rich superclusters (multiplicity $k > 4$)

(1) N_o	(2) N_{CL}	(3) α_C	(4) δ_C	(5) D_C h^{-1} Mpc	(6) Abell-ACO No.										(7) ID	(8) N_E
3	8	1.4	6.0	274	3	16	17	2694	2696e	2698	2700	2706			Pegasus - Pisces	1
4	4	1.9	-18.3	276	13	2682e	2710	2756e							Aquarius	126
5	5	2.9	-35.8	327	2715	2721	2730	2767	2772e							
6c	4	3.0	-62.7	299	2732e	2821e	4051e	4067								
9	22	7.3	-30.1	300	42	88	118	122	2726e	2751	2755–	2759e	2778	2780	Sculptor	3
					2798	2801	2804e	2811	2814	2829	2844	2878e	4021	4029e		
					4068	4074e										
10	17	8.6	-20.7	175	14	27	74	80	85	86	87	93e	114	117	Pisces - Cetus	6
					133	151	2716	2734	2800	2824	4053					
12c	4	9.8	-87.7	299	2757e	3037e	3299e	3650e								
16	4	12.5	-64.2	207	2810e	2819	2859	2864								15
18	6	13.2	-47.8	82	2731	2806	2836	2870	2877	2896					Phoenix	8
22c	5	15.6	-37.7	331	2823e	2838e	2865e	2871	2909e							
24	7	16.9	7.6	128	76	119	147	160	168	193	195				Pisces	16
26c	7	19.5	-18.6	320	166	183	185e	187e	197e	199e	2866e					
30	8	23.0	17.5	190	150	154	158	171	225	257	292	311			Pisces - Aries	17
31	4	24.1	-6.6	319	216	217	229	243								
34	6	27.7	-1.9	264	256	266	267e	268e	271e	277						18
38c	4	30.0	-26.5	330	2944e	2968e	2972e	2981e								
48	26	48.6	-49.3	191	3004	3009	3045e	3074	3078	3089	3093	3100	3104e	3106	Horologium -	27
					3108	3109	3110	3111	3112	3120	3122	3123	3125	3128	Reticulum	
					3135	3158	3164	3202	3225	3266						
49	5	48.9	-24.9	191	419	428	3094	3095	3151							27
50c	6	50.0	-69.9	314	3103e	3117e	3119e	3121e	3143e	3155e						
53c	12	55.5	-32.4	290	3118e	3146	3148e	3152e	3153e	3159e	3166e	3171e	3173e	3182e	Fornax - Eridanus	28
					3183e	3194										
54c	4	57.2	-32.1	218	3154e	3161e	3188e	3195e								29
59c	11	70.7	-33.6	298	3253e	3265e	3268e	3273e	3275e	3285e	3289e	3295	3297	3307e	Caelum	
					3325e											
62	5	74.3	8.5	305	515e	523	525e	529	532e							
63c	4	79.2	-49.4	314	3303e	3331e	3338e	3361e								
65	5	83.1	-41.3	228	3332	3336	3351e	3360	3379e							36, 37
66	4	86.4	-21.5	262	550e	3358e	3365	3368								38, 39
67	6	88.1	-28.1	114	548	3341	3367	3374	3381	3390					Lepus	41
71	5	100.9	69.5	314	554e	557e	561e	562	565							
76	4	131.2	28.4	244	690	692	699	722								47
82	4	151.2	-0.1	265	912	919	933	954								52
88	4	154.4	-7.7	159	970	978	979	993							Sextans	53
91	9	162.6	3.0	212	1024	1032	1066	1078	1080	1149	1171	1205	1238		Vela	58
93	9	165.2	19.9	96	999	1016	1139	1142	1177	1185	1228	1257	1267		Leo	56
95	4	167.6	38.6	218	1155	1187	1190	1203								55
100	10	173.7	-2.5	286	1189e	1200–	1248e	1296e	1364	1376e	1386	1389e	1399–	1404e	Leo A	64
107	8	175.9	10.0	316	1341	1342	1345	1354	1356	1372	1379e	1435e			Leo - Virgo	
109	8	176.8	54.9	173	1270	1291	1318	1377	1383	1436	1452	1507			Ursa Majoris	66
111	16	181.1	10.1	230	1262	1307	1337	1358	1385	1390	1424	1459	1474	1516	Virgo - Coma	70
					1526	1541	1552	1564	1569	1589						
114	16	181.9	64.3	310	1289	1302	1322	1366	1402	1406	1421	1432	1446	1477	Draco	
					1518	1559	1566	1621	1646	1674						
115c	5	182.6	-27.9	315	3495e	3498e	3506e	3514e	3516e							
118c	4	186.2	-15.1	274	1520e	1521	1535e	1585e								71
121c	4	193.3	-19.4	304	1605e	3529e	3534e	3539e								
124	34	195.8	-32.8	142	1631	1644	1709	1736	3490–	3492e	3497e	3500e	3505e	3509–	Shapley	80
					3524	3528	3530	3532	3542	3548e	3553	3554	3555			
					3556	3558	3559	3560	3561e	3562	3563	3564	3566	3570		
					3571	3572	3575	3577	3578							
126	6	195.9	-2.3	241	1620	1650	1651	1663	1692	1750						78
127	5	197.4	-30.4	217	1648	3531	3549e	3552e	3557–							76, 79
128	6	197.7	-33.1	39	1060	3526	3537	3565	3574	3581					Hydra - Centaurus	74
136	4	206.1	3.6	223	1773	1780	1784	1809								82
138	12	209.8	25.4	196	1775	1781	1795	1800	1825	1827	1828	1831	1861	1873	Bootes	83
					1898	1927										
147	4	220.6	54.8	294	1925	1962	1999	2000								86
150	10	223.6	21.1	324	1972	1976	1980	1986	1988	1997e	2001	2006	2017	2036	Bootes A	
154	4	228.0	4.9	224	2028	2029	2033	2066								89
155	4	228.4	-2.5	320	2035e	2045e	2050	2053								
157	6	229.1	31.7	323	2034	2046e	2049	2062	2069	2083						
158	8	230.8	29.7	208	2019	2061	2065	2067	2079	2089	2092	2124			Corona Borealis	90
160	12	236.2	18.5	105	2040	2052	2055	2063	2107	2147	2148	2151	2152	2162	Hercules	92
					2197	2199										
162	4	242.2	51.6	176	2149	2168	2169	2184								93
164	5	247.6	27.8	279	2175	2178	2200	2223	2228							
168	5	261.1	77.9	171	2248	2256	2271	2296	2309							96
170	7	276.9	69.6	249	2295	2301	2304	2308	2311	2312	2315					97
174	10	308.2	-35.0	259	3677	3681e	3682	3690e	3691	3693	3694	3695	3696	3705	Microscopium	101
178c	4	310.2	-80.7	257	3644e	3684e	3728e	3741e								
182c	4	319.8	-43.4	244	3751e	3755e	3756	3774e								
183c	6	320.6	-44.0	310	3749e	3754e	3757e	3767e	3772e	3775						
184	4	321.7	-21.6	325	2339	2347	3770e	3778								
188	9	327.6	-13.4	170	2361	2362	2366	2372	2382	2399	2401	2405e	2415		Aquarius - Cetus	108
189	4	327.9	-19.7	234	2370e	2378	2394	2412							Aquarius - Capricornus	111
190	5	328.4	-30.6	256	3795	3812	3813	3832	3837							106, 107
192	8	329.8	-55.4	215	3771	3785	3806	3822	3825	3849	3867e	3886			Grus - Indus	109
193	8	330.5	-9.9	239	2376	2377	2400	2402	2410	2420	2428	2448			Aquarius B	113
197	9	336.4	-51.3	279	3796–	3836e	3850e	3864	3877	3883	3911	3915e	3922		Grus	115

Table A1. continued

202	5	343.5	17.5	235	2458	2479	2516	2524	2564						119
205	19	346.1	-20.3	238	2456	2459	2462	2480	2492	2500	2502e	2523e	2528	2538	Aquarius 118, 120
					2539e	2541	2556	2566	2596e	2599	2600e	2605e	3985e		126
207	4	346.9	-14.1	306	2529	2533	2543	2559							
208	6	348.2	-42.0	57	3910	3963	3984	3987e	3998	4010					Piscis - Austrinus 121
209	7	348.5	-20.6	317	2546	2548	2554	2579	2583e	2586e	3964e				
210	6	350.4	-10.7	229	2511	2525	2569	2597	2638	2670					Aquarius A 122
211	4	351.7	15.3	120	2572	2589	2593	2657							Perseus - Pegasus A 123
213	6	353.6	21.9	188	2618	2622	2625	2626	2630	2637					Pegasus - Pisces B 125

The Table 1 gives data about superclusters. Columns are as follows:

(1) identification number of the supercluster in the catalogue; c stands for supercluster candidate;

(2) k – multiplicity of supercluster;

(3) and (4) α and δ (1950) – centre coordinates for supercluster;

(5): distance to the supercluster centre;

(6): numbers of supercluster members from the Abell - ACO catalogue;

(7): identification of supercluster;

(8) identification number of supercluster with common members from the catalogue by EETDA.

Comments to the Table. Supercluster center coordinates have been found as a mean value of supergalactic X, Y and Z coordinates of member clusters and then transformed to equatorial coordinates.

Clusters with estimated redshifts are marked with e; clusters with measured redshifts that do not belong to superclusters determined using only clusters with measured redshifts are marked with $-$.

Note – some superclusters were misordered in the Table 3 by EETDA; correct identification numbers in the column (8) are from the Table 2 in EETDA. We thank Prof. M. Kalinkov for turning our attention to these typos.